EL SEVIER

Contents lists available at ScienceDirect

# Science of the Total Environment

journal homepage: www.elsevier.com/locate/scitotenv



# Significant impact of heterogeneous reactions of reactive chlorine species on summertime atmospheric ozone and free-radical formation in north China



Xionghui Qiu <sup>a,b</sup>, Qi Ying <sup>c,\*</sup>, Shuxiao Wang <sup>a,b,\*\*</sup>, Lei Duan <sup>a,b</sup>, Yuhang Wang <sup>d</sup>, Keding Lu <sup>e</sup>, Peng Wang <sup>f</sup>, Jia Xing <sup>a,b</sup>, Mei Zheng <sup>g</sup>, Minjiang Zhao <sup>a,b</sup>, Haotian Zheng <sup>a,b</sup>, Yuanhang Zhang <sup>e</sup>, Jiming Hao <sup>a,b</sup>

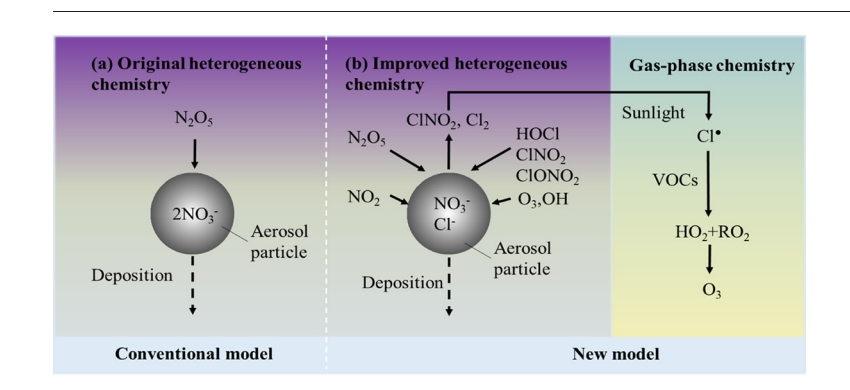
- <sup>a</sup> State Key Joint Laboratory of Environmental Simulation and Pollution Control, School of Environment, Tsinghua University, Beijing 100084, China
- <sup>b</sup> State Environmental Protection Key Laboratory of Sources and Control of Air Pollution Complex, Beijing 100084, China
- <sup>c</sup> Zachry Department of Civil Engineering, Texas A&M University, College Station, TX, United States
- <sup>d</sup> School of Earth and Atmospheric Sciences, Georgia Institute of Technology, Atlanta, GA 30332, United States
- e State Key Joint Laboratory of Environmental Simulation and Pollution Control, College of Environmental Sciences and Engineering, Peking University, Beijing, China
- f Department of Civil and Environmental Engineering, The Hong Kong Polytechnic University, 999077, Hong Kong, China
- g SKL-ESPC and BIC-ESAT, College of Environmental Sciences and Engineering, Peking University, Beijing 100871, China

#### HIGHLIGHTS

# This work represents the first high resolution regional modeling to quantify the impact of chlorine chemistry on the oxidation capacity in a polluted urban atmosphere.

- These heterogeneous reactions of reactive chlorine species increased the O<sub>3</sub>,
   OH, HO<sub>2</sub> and RO<sub>2</sub> concentrations significantly for some regions in the Beijing-Tianjin-Hebei (BTH) area.
- The heterogeneous reactions of O<sub>3</sub> are the most important source of Cl<sub>2</sub> (81%).

#### GRAPHICAL ABSTRACT



# ARTICLE INFO

Article history: Received 21 April 2019 Received in revised form 23 July 2019 Accepted 23 July 2019 Available online 24 July 2019

Editor: Jianmin Chen

Keywords:
Ozone
Heterogeneous reaction
Reactive chlorine species

# ABSTRACT

Heterogeneous reactions of N<sub>2</sub>O<sub>5</sub>, O<sub>3</sub>, OH, ClONO<sub>2</sub>, HOCl, ClNO<sub>2</sub>, and NO<sub>2</sub>, with chlorine-containing particles are incorporated in the Community Multiscale Air Quality (CMAQ) model to evaluate the impact of heterogeneous reactions of reactive chlorine species on ozone and free radicals. Changes of summertime ozone and free radical concentrations due to the additional heterogeneous reactions in north China were quantified. These heterogeneous reactions increased the O<sub>3</sub>, OH, HO<sub>2</sub> and RO<sub>2</sub> concentrations by up to 20%, 28%, 36% and 48% for some regions in the Beijing-Tianjin-Hebei (BTH) area. These areas typically have a larger amount of NOx emissions and a lower VOC/NOx ratio. The zero-out method evaluates that the photolysis of ClNO<sub>2</sub> and Cl<sub>2</sub> are the major contributors (42.4% and 57.6%, respectively) to atmospheric Cl• in the early morning hours but the photolysis of Cl<sub>2</sub> is the only significant contributor after 10:00 am. The results highlight that heterogeneous reactions of reactive chlorine species are important to atmospheric ozone and free-radical formation. Our study also suggests that the on-going NOx emission controls in the NCP region with a goal to reduce both O<sub>3</sub> and secondary nitrate can

<sup>\*</sup> Corresponding author.

<sup>\*\*</sup> Correspondence to: S. Wang, State Key Joint Laboratory of Environmental Simulation and Pollution Control, School of Environment, Tsinghua University, Beijing 100084, China. E-mail addresses: qying@civil.tamu.edu (Q. Ying), shxwang@tsinghua.edu.cn (S. Wang).

also have the co-benefit of reducing the formation Cl• from ClNO<sub>2</sub> and Cl<sub>2</sub>, which may also lead to lower secondary organic aerosol formation and thus the control of summertime PM<sub>2.5</sub> in the region.

© 2019 Elsevier B.V. All rights reserved.

#### 1. Introduction

Atmospheric chlorine radicals generated from chlorofluorocarbons (CFCs) are widely known for their active role in the destruction of the stratospheric ozone layer (Butchart and Scaife, 2001). While CFCs are generally non-reactive in the lower troposphere, high concentrations chlorine gas (Cl<sub>2</sub>) and reactive chlorine species have been detected in coastal cities and major urban areas and even unexpectedly in the lower atmosphere in the remote Arctic region (Von Glasow, 2010: Osthoff et al., 2008: Liao et al., 2014). The Cla and other reactive chlorine species, such as hypochlorous acid (HOCl), nitryl chloride (ClNO<sub>2</sub>) and chlorine nitrate (ClONO<sub>2</sub>), are expected to enhance the atmospheric oxidation capacity when they are photolyzed to generate the highly reactive chlorine radicals (Cl•) (see Table S1) (Thornton et al., 2010; Oum et al., 1998; Wang et al., 2005), accelerating the oxidation of volatile organic compounds (VOCs). The faster oxidation of VOCs by Cl• simultaneously enhances the production of  $O_3$  and organic peroxy radicals ( $RO_2$ ) as well as the recycling of hydroxyl (OH) and hydroperoxyl (HO<sub>2</sub>) radicals (Wang et al., 2007; Graedel and Keene, 1995; Finley and Saltzman, 2006). In some field measurements, the occurrence of high concentrations of O<sub>3</sub>, OH, HO<sub>2</sub> and RO<sub>2</sub> are positively correlated with increasing Cl<sub>2</sub> and other chlorine compounds (Liu et al., 2017), indicating that tropospheric chlorine species are important in determining the overall atmospheric reactivity for  $O_3$  formation.

Most current chemical transport models (CTMs) have difficulties in simulating the concentrations of chlorine compounds and thus correctly quantifying the effects of chlorine chemistry on atmospheric reactivity and O<sub>3</sub> formation because the models have inadequate representation of the chlorine chemistry, especially the heterogeneous reactions involving the particulate chloride (PCI) and the production of reactive gaseous chlorine species (Finlayson-pitts et al., 1989; Thornton and Abbatt, 2005). In most CTMs the heterogeneous uptake of dinitrogen pentoxide (N<sub>2</sub>O<sub>5</sub>) on aqueous aerosols and water droplets only leads to the production of particulate nitrate, regardless of the concentrations of PCl. However, recent studies suggest that N<sub>2</sub>O<sub>5</sub> produces nitrate and CINO<sub>2</sub> on chlorine-containing aerosol surfaces, such as sea salt particles (Li et al., 2016; Osthoff et al., 2008; Yu et al., 2010). Various studies added this reaction into the model and the reported increase in O<sub>3</sub> in regional photochemical modeling studies for northern China varied from 3 to 6% by Sarwar et al. (2014) to ~11.5% by Zhang et al. (2017). Box model simulations by Wang et al. (2016) for southern China and by Liu et al. (2017) for northern China concluded that ozone production rate increased by 11-41% and 19%, respectively. The cause of the large variations in the model assessments is unclear and needs to be further investigated.

In addition to ClNO<sub>2</sub> production through the N<sub>2</sub>O<sub>5</sub> reaction, other heterogenous reactions related to reactive chlorine species have been reported in the literature. For example, laboratory observations found that Cl<sub>2</sub> production could occur from irradiated mixtures of O<sub>3</sub> and PCl (Behnke and Zetzsch, 1989; Keene et al., 1990). Sander and Crutzen (1996) and Gebel and Finlayson-Pitts (2001) suggested that Cl<sub>2</sub> could also be produced by heterogeneous uptake of HOCl, OH, ClNO<sub>2</sub> and ClONO<sub>2</sub> on particle surface under different atmospheric conditions. Abbatt and Waschewsky (1998) concluded that gaseous NO<sub>2</sub> could also react with chlorine-containing aerosol to produce reactive chlorine species. These missing chlorine heterogeneous reactions contribute to the additional formation of Cl• from Cl<sub>2</sub> during daytime hours but the amount of Cl<sub>2</sub> that can be generated from these reactions and their

synergetic effects on O<sub>3</sub> and peroxy radical concentrations in a polluted urban atmosphere have not been subject to rigorous assessments using a unified comprehensive modeling framework.

Atmospheric chlorine in polluted areas mainly originates from combustion sources. According to the chlorine emission inventory developed by the International Global Atmospheric Chemistry Program's Global Emissions Inventory Activity (GEIA) based on the year 1990, biomass burning (42%), coal combustion (37%), and waste incineration (21%) were the major sources of inorganic chlorine in China (Keene et al., 1999). A number of local measures also detect high content of PCl in PM<sub>2.5</sub> (particulate matter with an aerodynamic diameter <2.5) μm) from power plants, residential combustion, and biomass burning sources (Li et al., 2017; Qiu et al., 2016; Shen et al., 2010). Coal and biomass burning are regarded as the culprit of the severe air pollution events in north China. According to statistics (Cai et al., 2017), about 300 megatons (MT) of coal is consumed for industrial production and residential heating and nearly 40 MT of biomass is burned during post-harvest in north China in 2014. These two sources lead to 35 Gg of particulate chlorine emissions in the North China Plain region. Consequently, Liu et al. (2017) observed high concentrations of Cl<sub>2</sub> (up to 450 pptv) and ClNO<sub>2</sub> (~3640 pptv) in June 2014 in Wangdu, a city in the polluted NCP. Thus, it's necessary to explore the effects of high concentrations of Cl2, CINO2 and other reactive chlorine species on the atmospheric oxidation capacity in polluted urban areas.

In this study, a three-dimensional (3D) CTM, the Community Multiscale Air Quality (CMAQ) model, is improved to include a more complete description of the gas phase reactions of the chlorine species and the heterogeneous reactions associated with the production and destruction of these reactive chlorine species. The updated model is applied to study summer ozone concentrations in north China. This work represents the first regional CTM modeling study that includes a complete treatment of gas phase and heterogeneous chlorine chemistry to evaluate their impacts on chlorine of  $\rm O_3$ ,  $\rm HO_x$  (OH + HO<sub>2</sub>) and organic peroxy radicals (RO<sub>2</sub> = RO<sub>2</sub>C + RO<sub>2</sub>XC + MEO<sub>2</sub>) in north China. The results of this study also have significant implications for designing future emission control strategies.

# 2. Methods

# 2.1. Heterogeneous chemistry for reactive chlorine species

CMAQ version 5.0.1 is used as the framework to implement the chlorine mechanisms. The SAPRC-11 gas-phase chemical mechanism with an extension of comprehensive chlorine gas-chemistry is implemented in the model (detailed description in Table S1) (Ying et al., 2015). In the original CMAQ model, the heterogeneous uptake of  $N_2O_5$  on wet aerosol surfaces occurs via reaction (R1):

$$N_2O_5(g) + H_2O(aq) \rightarrow 2HNO_3(aq) \tag{R1}$$

In this study, gaseous ClNO<sub>2</sub> production on the chlorine-containing aerosols via reaction (R2) is considered (Roberts et al., 2009; Sarwar et al., 2012):

$$N_2O_5(g) + Cl^-(aq) \rightarrow HNO_3(aq) + ClNO_2(g)$$
 (R2)

Reactions R1 and R2 are represented in the model as an overall reaction (R3):

$$\begin{array}{l} N_2O_5(g) + (1-\eta)H_2O(aq) + \eta Cl^-(aq) {\rightarrow} (2-\eta)HNO_3(aq) \\ + \eta ClNO_2(g) \end{array} \tag{R3}$$

in which the parameter  $\eta$  represents the yield of ClNO<sub>2</sub> and is calculated by Eq. (1) (Bertram and Thornton, 2009):

$$\eta = \left(1 + \frac{[H_2O]}{483 \times [Cl^-]}\right)^{-1} \tag{1}$$

In the above formula,  $[H_2O]$  and  $[Cl^-]$  are the molarities of liquid water and chloride in aerosol volume (mol m<sup>-3</sup>).

Additional heterogeneous reactions involving reactive chlorine species such as  $\text{Cl}_2$  are included in the CMAQ model based on a literature search of experimental studies. A summary of these additional reactions is given below, followed by a discussion of the parameterization of their uptake coefficients.

It was observed in previous experiments that the concentration of  $\text{Cl}_2$  increased rapidly from irradiated mixtures of  $\text{O}_3$  and chloride-containing aerosols (Knipping et al., 2000), which could be explained by the heterogeneous uptake of gas phase  $\text{O}_3$  on the particle surface via reaction (R4):

$$2Cl^{-}(aq) + O_{3}(g) + H_{2}O(aq) \rightarrow Cl_{2}(g) + 2OH^{-}(aq) + O_{2}(g) \tag{R4} \label{eq:R4}$$

Knipping et al. (2000) suggested that the formation of  $Cl_2$  in a chamber experiment that exposed chloride-containing aerosols to OH could be modeled with the heterogeneous reaction of gaseous OH with particulate  $Cl^-$ . The reaction intermediates  $OH \cdot Cl^-$  subsequently self-reacts to produce  $Cl_2$ , as shown in reactions R5 and R6 (Faxon et al., 2015; George and Abbatt, 2010):

$$OH(g) + Cl^{-}(aq) \rightarrow OH \cdot Cl^{-}(aq)$$
(R5)

$$OH \cdot Cl^{-}(aq) + OH \cdot Cl^{-}(aq) \rightarrow Cl_{2}(g) + 2OH^{-}(aq)$$
 (R6)

Heterogeneous reactions of ClONO<sub>2</sub> and HOCl at the acidic particle surface can also lead to Cl<sub>2</sub> production (Deiber et al., 2004; Pratte and Rossi, 2006), as shown in reactions R7 and R8, respectively:

$$CIONO_2(g) + Cl^-(aq) + H^+(aq) \rightarrow Cl_2(g) + HNO_3(g)$$
 (R7)

$$HOCl(g) + Cl^{-}(aq) + H^{+}(aq) \rightarrow Cl_{2}(g) + H_{2}O(aq)$$
 (R8)

For  $CINO_2$ , the production of  $Cl_2$  was shown to follow reaction R9 in acidity condition (pH < 2) and decompose to produce PCl at higher pH as shown in R10 (Riedel et al., 2012; Rossi, 2003).

$$CINO_2(g) + Cl^- (aq) + H^+(aq) \rightarrow Cl_2(g) + HONO(aq)$$
 (R9)

$$CINO_2(g) \rightarrow Cl^- + NO_3^- + 2H^+$$
 (R10)

Lastly, as shown in reaction R11, the surface uptake of  $NO_2$  on chlorinated particle surface was considered to produce gaseous ClNO (Abbatt and Waschewsky, 1998), an intermediate species which subsequently produces Cl• radicals through gas phase reactions (the reactions M03 and M21 in Table S1).

$$2NO_2(g) + Cl^-(aq) \rightarrow ClNO(g) + NO_3^-(aq)$$
 (R11)

In summary, the heterogeneous reactions (R3–R11) involving gaseous  $N_2O_5$ ,  $O_3$ , OH, ClONO<sub>2</sub>, HOCl, ClNO<sub>2</sub>, and NO<sub>2</sub> uptake on particle surface are included in the revised CMAQ model. These irreversible heterogeneous reactions are treated as gas phase diffusion limited first-

order reactions, with the overall reaction rate is parameterized according to Ying et al. (2015) as shown in Eq. (2),

$$R = -\frac{d\rho_m}{dt} = \frac{1}{4} \gamma \nu \rho_m S \tag{2}$$

where  $\gamma$  is the uptake coefficient of the gas phase species;  $\nu$  is its thermal velocity (m s  $^{-1}$ );  $\rho_{\rm m}$  is the species concentration (µg m  $^{-3}$ ) in the gas phase; and S is the aerosol surface area concentration (m  $^2$  m  $^{-3}$ ). The values of  $\rho_{\rm m}$  and S are obtained from the gas and aerosol phase simulations, and the  $\gamma$  for air pollutants are based on the laboratory measurements reported in the literature, which are summarized below.

The uptake coefficient  $\gamma$  for N<sub>2</sub>O<sub>5</sub> in the original CMAQ model was based on the parameterization of Davis et al. (2008), which increases with increasing of RH and decreasing of T and depends on the particulate concentrations of (NH<sub>4</sub>)<sub>2</sub>SO<sub>4</sub>, NH<sub>4</sub>HSO<sub>4</sub> and NH<sub>4</sub>NO<sub>3</sub>. However, this parameterization does not include particle chlorine, which was shown to affect the uptake coefficient of N<sub>2</sub>O<sub>5</sub> in several experimental studies (McDuffie et al., 2018; Sarwar et al., 2014). Thus, the parameterization by Bertram and Thornton (2009), as shown in Eq. (3), is used in this study,

$$\gamma_{N_2O_5} = \begin{cases} 0.02, for frozen aerosols, \\ 3.2 \times 10^{-8} K_f \left[ 1 - \left( 1 + \frac{6 \times 10^{-2} [\text{H}_2\text{O}]}{[\text{NO}_3^-]} + \frac{29[\text{Cl}^-]}{[\text{NO}_3^-]} \right)^{-1} \right] \end{cases}$$
(3)

In the above equation,  $K_{\rm f}$  is a parameterized function based on molarity of water:  $K_{\rm f}=1.15\times 10^6(1-e^{-0.13[{\rm H_2O}]})$ . NO $_3^-$  and Cl $^-$  concentrations are also in molarity. The  $\gamma$  value of O $_3$  used in this study follows the suggestions by Keene et al. (Keene et al., 1990), with a daytime value of  $10^{-3}$  and a nighttime value of  $10^{-5}$ . Several laboratory measurements reported that the  $\gamma$  value of OH was strongly associated with RH and ranged from 0.1 to 0.2 (George and Abbatt, 2010; Laskin et al., 2006). The IUPAC (International Union of Pure and Applied Chemistry) recommends that OH heterogeneous uptake  $\gamma$  be parameterized as a function of the molarity of Cl $^-$  (available at http://iupac.poleether.fr/htdocs/datasheets/pdf/OH\_halide\_solutions\_VI.

A2.1.pdf) as shown in Eq. (4):

$$\gamma = \min\left(0.04 \times \frac{[\mathit{Cl}^{-}]}{1000 \times \mathit{M}}, 1\right) \tag{4}$$

where M is the volume of liquid water in aerosol volume ( $m^3 m^{-3}$ ). This equation was derived based on experiments using aqueous sea salt aerosol and is used in this study to calculate the uptake coefficient of OH on wet aerosol surfaces. HOCl reacts on aerosol with a  $\gamma$  ranging from  $0.39 \times 10^{-3}$  to  $1.79 \times 10^{-3}$  at a RH at 40%~85% (Pratte and Rossi, 2006). The average value of  $1.09 \times 10^{-3}$  is used in this work. The uptake coefficient of CIONO2 used in this study is a constant value of 0.16 according to the suggestion of Gebel and Finlayson-Pitts (2001), which is lower than the initial uptake coefficient of up to 0.42 determined using fresh sea salt aerosols but higher than the lower limit of 0.02-0.04 for aged sea salt aerosols. The uptake coefficient of ClNO<sub>2</sub> for reaction R9 depends on particle acidity (Roberts et al., 2008). For neutral particles, the reported  $\gamma$  ranges from  $0.3 \times 10^{-6}$  to  $5 \times 10^{-6}$ , and the average value of  $2.65 \times 10^{-6}$  is used in this study. For acidic aerosols, a much higher value of  $\gamma$  (6 × 10<sup>-3</sup>) is used. The  $\gamma$  of NO<sub>2</sub> takes a constant value of 10<sup>-4</sup>, following the study of Abbatt and Waschewsky (1998).

# 2.2. Model setup

The CMAQ model with the modified heterogeneous chlorine chemistry is applied to simulate the regional concentrations of Cl<sub>2</sub>, PCl and related gaseous chlorine species (ClNO<sub>2</sub>, HCl and ClONO<sub>2</sub>,

etc.) and evaluate the impact of chlorine chemistry on ozone and free radicals in northern China. The model setup, preparation of emissions (without chlorine) and meteorological inputs have been described in previous publications (Cai et al., 2017; Chang et al., 2017). Three-level nested domains with spatial resolutions of 36 km, 12 km, and 4 km are used in this work (for the innermost domain, see Fig. S2). The chloride emission inventory, including inorganic hydrogen chloride (HCl) and fine particulate chloride, is obtained from Fu et al. (2018). Two cases, a base case (BASE) without chlorine heterogeneous chemistry and a case with chlorine heterogeneous chemistry (HET) are compared to reveal the differences due to the inclusion of the heterogeneous reactions. In both cases, emissions of HCl and PCl and the extended gas-phase chlorine chemistry are included.

#### 3. Results

#### 3.1. Model performance evaluation

Predicted  $O_3$ ,  $SO_2$ ,  $NO_2$  and  $PM_{2.5}$  concentrations from the BASE case simulation are evaluated against monitoring data in 13 major cities in the Beijing-Tianjin-Hebei (BTH) region (Table S2). The average NMB/NME values for  $O_3$ ,  $NO_2$  and  $PM_{2.5}$  across the 13 cities are -15%/31.5%, 0.5%/31% and -16%/32%, respectively, which are similar to the model performance reported in previous modeling studies in this region (Chang et al., 2017).

Simulated hourly Cl<sub>2</sub> and ClNO<sub>2</sub> concentrations from 12 to 30 June 2014, are compared with observations measured by Liu et al. (2017) using a Chemical Ionization Mass Spectrometer (CIMS) in Wangdu (38.67°N, 115.20°E). Fig. 1(a) and (b) show that the simulated Cl<sub>2</sub> and CINO<sub>2</sub> concentrations in the BASE case are close to zero, indicating that emissions HCl and PCl and gas phase chlorine chemistry alone is not enough to explain the observed Cl<sub>2</sub> and ClNO<sub>2</sub> concentrations. By contrast, the HET case predicts significantly higher Cl2 and ClNO2 concentrations, which reduce the NMB and NME of both species (Table S3). However, the simulated Cl<sub>2</sub> mixing ratio is higher than the observations, while the simulated ClNO<sub>2</sub> mixing ratio is underestimated. The possible causes are further discussed in Section 4. Direct measurements of PCl are not available at this site. However, PCl measurements are available at the Liulihe monitoring site in Beijing (39.65°N, 116.25°E, about 120 km from the Wangdu site, see Fig. S2) from July 24 to July 31 in 2014. PCl predictions from both the BASE and HET simulations agree well with the observed high concentrations throughout the week (see Panel 1c). Time series of O<sub>3</sub> at Wanliu (a state controlling air sampling site in Beijing, 39.96°N, 116.30°E) are shown in Fig. 1(d) as an example to illustrate its hour-to-hour variations. On average, the HET case reduces the NMB and NME by 2.4%. Concentrations of another chlorine species ClONO<sub>2</sub> have not been measured in the troposphere. A plot of the episode average hourly ClONO<sub>2</sub> concentrations and a brief discussion is included in Fig. S1.

During the summer 2014 field campaign,  $N_2O_5$  and HCl concentrations were not measured. In order to more comprehensively evaluate the model, an additional set of simulation was performed for June 11 to 15, 2017, during which  $N_2O_5$ ,  $Cl_2$ ,  $ClNO_2$ , and HCl concentrations were measured at the Institute of Atmospheric Physics (IAP) in urban Beijing (Fig. S2) by Zhou et al. (2018) using CIMS. For this episode, the averaged concentrations of  $ClNO_2$ ,  $N_2O_5$ , and HCl are well represented by the model even though the concentrations are under-predicted. The detailed process sees our previous study (Qiu et al., 2019). The NMB/NME values for  $ClNO_2$  in the HET case in Wangdu are -58%/64%, which are similar or slightly better than the those reported by Li et al. (2016) (-50%/109%) for southern China and Simon et al. (2009) (NME~-80%) for Houston, USA. That's because the emission of chloride compound in China is significant higher than that in USA.

3.2. Impacts of chlorine heterogeneous chemistry on ozone and free-radical

The heterogeneous production of Cl<sub>2</sub> and ClNO<sub>2</sub> also leads to increases in CI and OH radical concentrations, causing a significant increase in the oxidation capacity of the urban atmosphere. Fig. 2 shows the regional distribution of monthly concentrations of Cl•, O<sub>3</sub>, OH, HO<sub>2</sub> and RO<sub>2</sub> from the HET simulation and the relative difference between the BASE and HET simulations for July 2014. The monthly average Cl• concentrations in the HET simulation ranges from 10<sup>3</sup> to 10<sup>4</sup> molecules cm<sup>3</sup>. Significant increases in Cl• concentrations are found in most regions, as high as 3000-7000 times in eastern and southern areas of the Beijing-Tianjin-Hebei (BTH) region and 100-400 times in other areas, indicating the important role of chlorine heterogeneous chemistry on Cl. production. Although direct measurements of Cl. concentrations are not available, some other simulations using box-models constrained by observed Cl<sub>2</sub> and/or ClNO<sub>2</sub> roughly agree with the predictions from this study. For example, averaged concentration Cl• of about  $4 \times 10^4$  molecules cm<sup>-3</sup> from 11 June to 1 July in 2014 in north China were predicted by Liu et al. (2017) and approximately 0.85  $\times$  10<sup>4</sup> molecules cm<sup>-3</sup> of morning peak Cl• averaged from 15 May to 15 June in 2010 in Los Angeles were estimated by Young et al. (2014).

Higher concentrations of Cl• lead to higher concentrations of RO<sub>2</sub> and HO<sub>2</sub> radicals due to the reactions of Cl• with VOCs (M24-M31 in Table S1), as shown in Fig. 2(c-d) and (e-f). Higher relative increases of RO<sub>2</sub> (>40%) and HO<sub>2</sub> (>30%) occur in eastern and southern BTH where the RO<sub>2</sub> concentrations are low in the BASE case. These areas typically have a larger amount of NOx emissions and thus a lower VOC/NOx ratio (Cai et al., 2017; Zhao et al., 2018). The increased Cl<sub>2</sub> and Cl radical lead to faster VOC oxidation, and thus higher concentrations of HO2 and RO<sub>2</sub> radicals. While these radicals can contribute to the ozone formation by recycling NO to NO<sub>2</sub>, their impacts are highest in regions where O<sub>3</sub> formation is VOC-limited. In NOx-limited regions, where  $O_3$  formation rate is mostly controlled by the NO<sub>2</sub> photolysis rate, their impacts on O<sub>3</sub> are diminished. Spatial distributions of OH and its increase are similar to that of  $HO_2$  with a relative increase of up to approximately 30% in the eastern and southern BTH areas, due to the sequential conversion from RO<sub>2</sub> and HO<sub>2</sub> and to OH. Fig. 2(i-j) show that O<sub>3</sub> concentrations from the HET case are higher than those from the BASE case. The higher relative increases (10%-25%) also occur in the southern BTH region.

Take an observation site with high growth rates of ozone and free radicals concentrations as an example (red circle in Fig. 2(j), located in Handan), hourly O<sub>3</sub>, OH, HO<sub>2</sub> and RO<sub>2</sub> concentrations in July 2014 from the BASE and the HET cases are compared in Fig. 3 in order to have an insight into their association with Cl•. The temporal variations of O<sub>3</sub>, OH, HO<sub>2</sub> and RO<sub>2</sub> concentrations are similar, with the highest values occur at 13:00-14:00 local time. Moreover, the relative difference of hourly O<sub>3</sub>, OH, HO<sub>2</sub> and RO<sub>2</sub> between the HET and BASE case shows a bimodal distribution with two peaks on 7:00-8:00 and 18:00-19:00, with peak values of 45.7% and 22.8% (O<sub>3</sub>), 88.9% and 30.1% (OH), 148% and 72.1% (HO<sub>2</sub>), and 152% and 99.0% (RO<sub>2</sub>). This bimodal distribution matches the bimodal distribution of the concentrations of Cl• (Fig. 4). At early morning with the appearance of sunlight, Cl• quickly increases due to the photolysis of Cl<sub>2</sub> and reactive chlorine species accumulated at night. Its reaction with VOCs prompts the production of O<sub>3</sub>, OH, HO<sub>2</sub> and RO<sub>2</sub>. However, the concentration of Cl• is quickly depleted and accordingly the relative changes of O<sub>3</sub>, OH, HO<sub>2</sub> and RO<sub>2</sub> between the two cases reduce. Later during the day, stronger solar radiation and higher O<sub>3</sub> prompt and sustain the production of Cl• from Cl<sub>2</sub> leading to higher O<sub>3</sub> and radicals in the HET case. After 18:00, the photolysis rate of Cl<sub>2</sub> and reactive chlorine species recede, decreasing the growth rates of Cl•, O<sub>3</sub>, OH, HO<sub>2</sub> and RO<sub>2</sub>.

The hourly HONO concentrations are not available at this work. However, Tan et al. (2017) detected that the averaged concentration of HONO was about 0.8 ppb in the daytime and 1.5 ppb in the nighttime measured at Wangdu site from June 7 to July 8, 2014. By contrast, we find that the simulated HONO concentration estimated by original

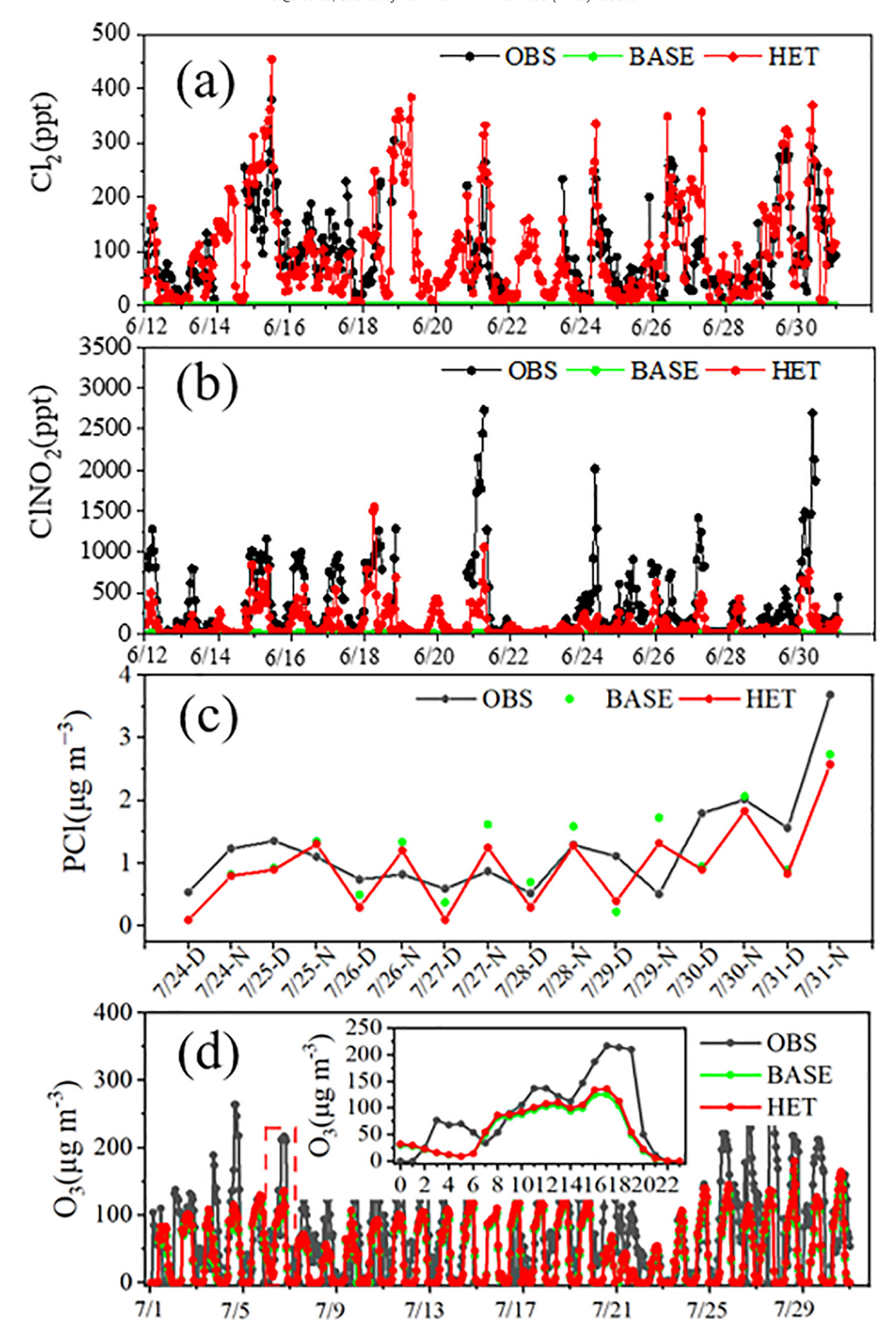


Fig. 1. Observed and simulated (a) hourly Cl<sub>2</sub> at Wangdu, (b) hourly ClNO<sub>2</sub> at Wangdu, (c) day and nighttime particulate chloride (PCl) at Liulihe and (d) hourly ozone at Wanliu using the original (BASE) and improved CMAQ (HET) (-D: daytime, -N: nighttime). The results of panels (a) and (b) are for June 12 to 30, 2014. The inset figure in panel (d) shows the hourly concentration time series on July 6.

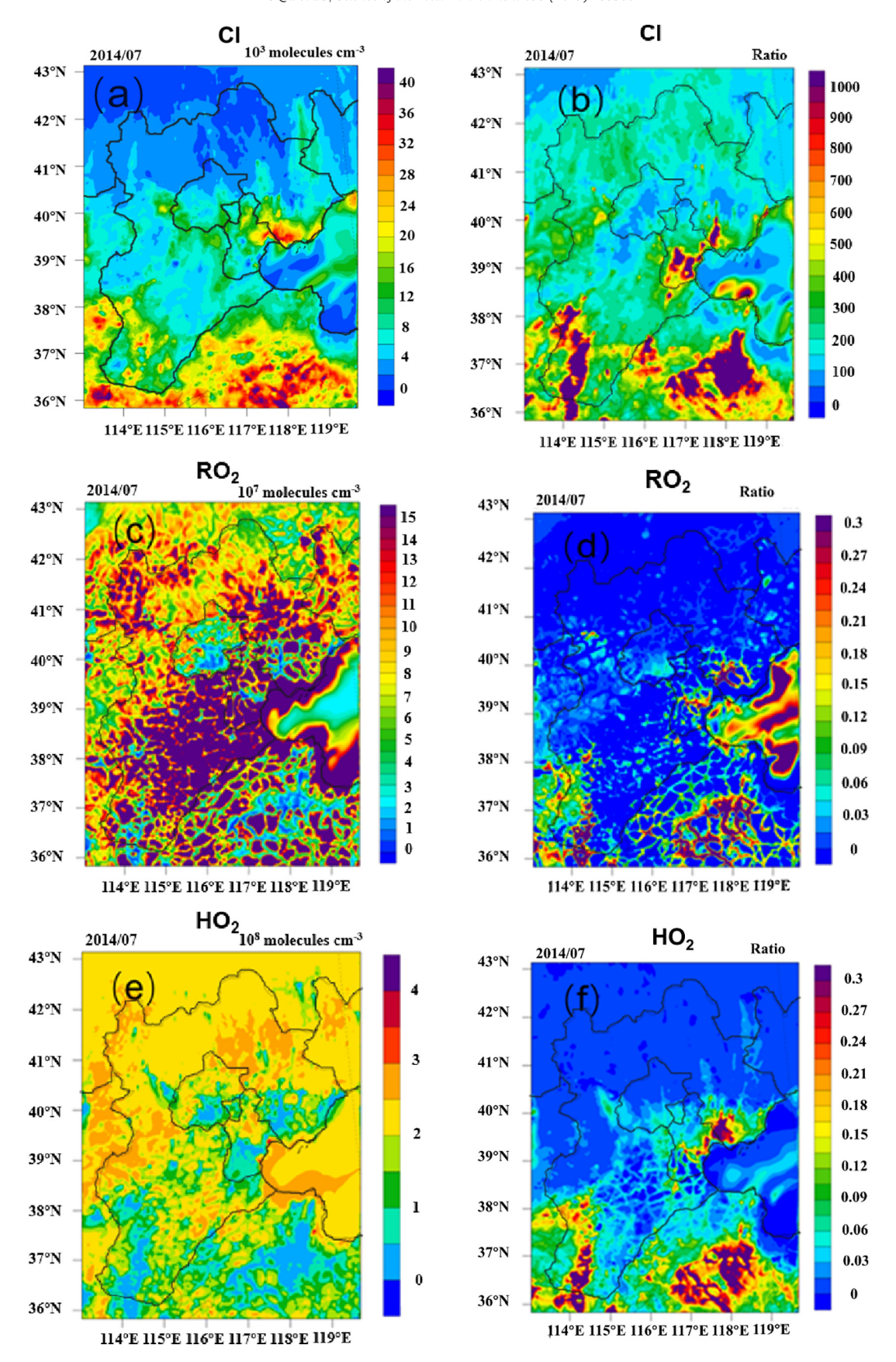


Fig. 2. Spatial distribution of simulated Cl, RO<sub>2</sub> HO<sub>2</sub>, OH, and O<sub>3</sub> using improved CMAQ (HET case, left column) and the relative changes between original (BASE case) and improved CMAQ [(HET-BASE)/BASE, right column]. The results are based on averaged concentrations during the entire month of July 2014.

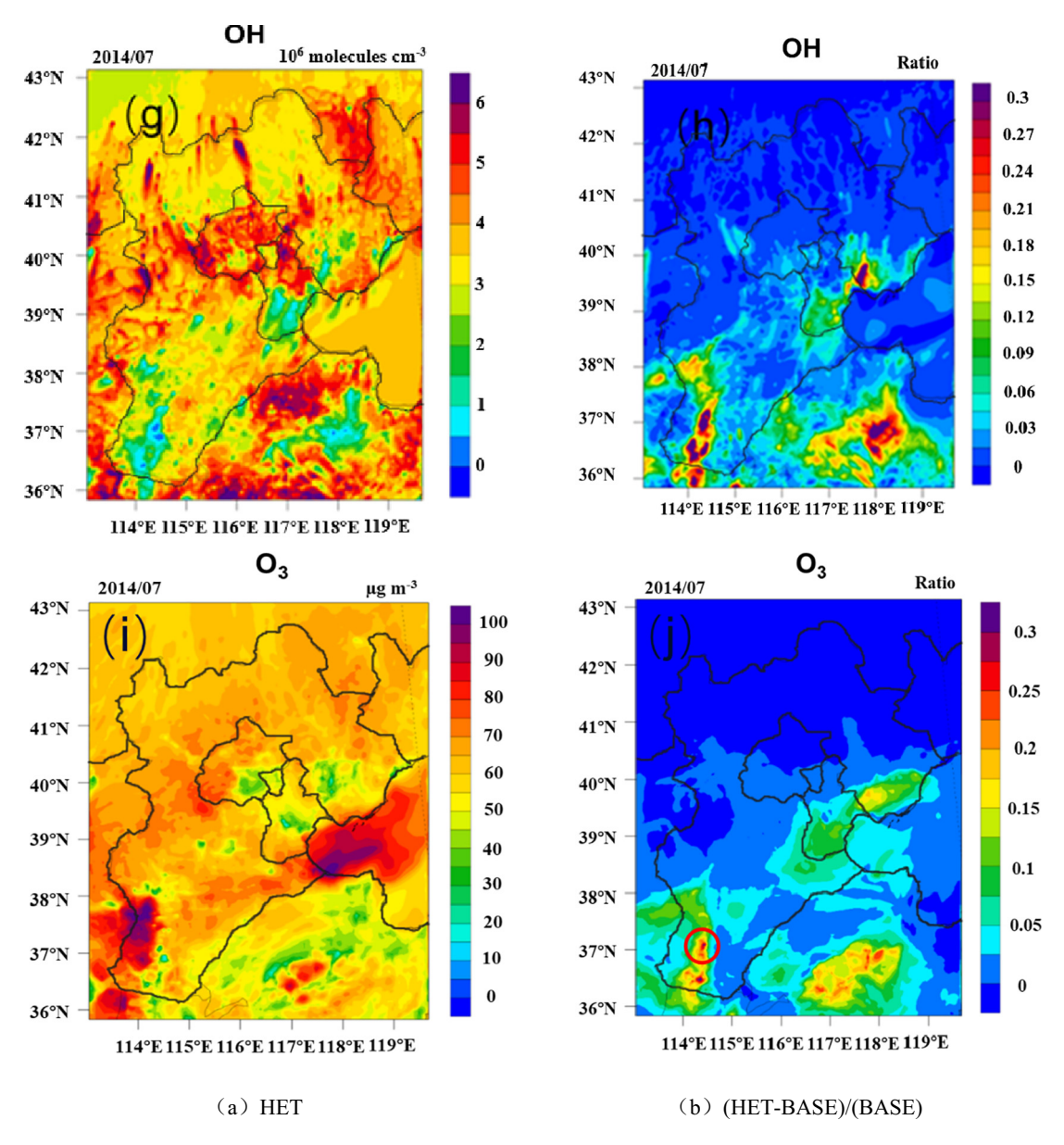


Fig. 2 (continued).

CMAQ is overestimated (about 3 ppb in the nighttime and 1 ppb in the daytime). Since the reaction of  $NO_2$  with PCl is improved ( $NO_2$  reacts with  $H_2O$  in original model), the simulated HONO concentration decreases to 1.2 ppb in nighttime and 0.7 ppb in the daytime, which indicates that this improved model is suitable for applying in this work. A sensitivity simulation is designed by revising the  $NO_2$  with  $H_2O$  or not (aim to evaluate the difference of OH generated by HONO and ClNO photolysis). The results show that this improvement can elevate the OH concentration by about 1.3 times in the daytime but decrease by 2 times in the nighttime, concluding that this improvement is more favorable for producing OH in the daytime.

The impacts on peak hour  $O_3$  levels is higher than the study by Sarwar et al. (2012) (~6%) and comparable to the study by Li et al. (2016) (~17%). This is expected because higher daytime  $Cl_2$  and  $Cl^4$  with the inclusion of these additional heterogeneous reactions lead to a large increase in the OH,  $HO_2$  and  $RO_2$  concentrations. Additionally, Sarwar et al. (2012) only evaluated the impact of sea-salt heterogeneous reactions on the improvement of  $O_3$  concentration, the anthropogenic emission of chlorine species are not involved.

The nighttime increase of  $O_3$  is mainly due to the increased  $O_3$  during daytime hours. In regions without large direct NO emissions to titrate  $O_3$  at night, elevated  $O_3$  concentration can persist. Regional transport of higher  $O_3$  from other regions (which are also due to daytime chlorine chemistry) can also lead to higher  $O_3$  concentrations in downwind area at night. As the  $Cl_2$  generated from heterogeneous reactions does not react at night based on the current mechanism, the slight increase of  $RO_2$ ,  $HO_2$  and OH at night shown in Fig. 3 is not due to chlorine chemistry. Instead, it is mainly due to increased gas phase  $O_3$  reaction rates with unsaturated organic compounds such as alkenes and monoterpenes in the HET case.

# 3.3. Sources of chlorine radical

Previously, most literature reported that Cl• was originated from the photolysis of ClNO<sub>2</sub> (e.g. Young et al. (2014) and Li et al. (2016)). However, direct observations of  $Cl_2$  made by Liu et al. (2017) showed that  $Cl_2$  peaks at noon time with concentrations around 100 ppt, suggesting that the  $Cl_2$  photolysis can be a major source of Cl•. While the contributions

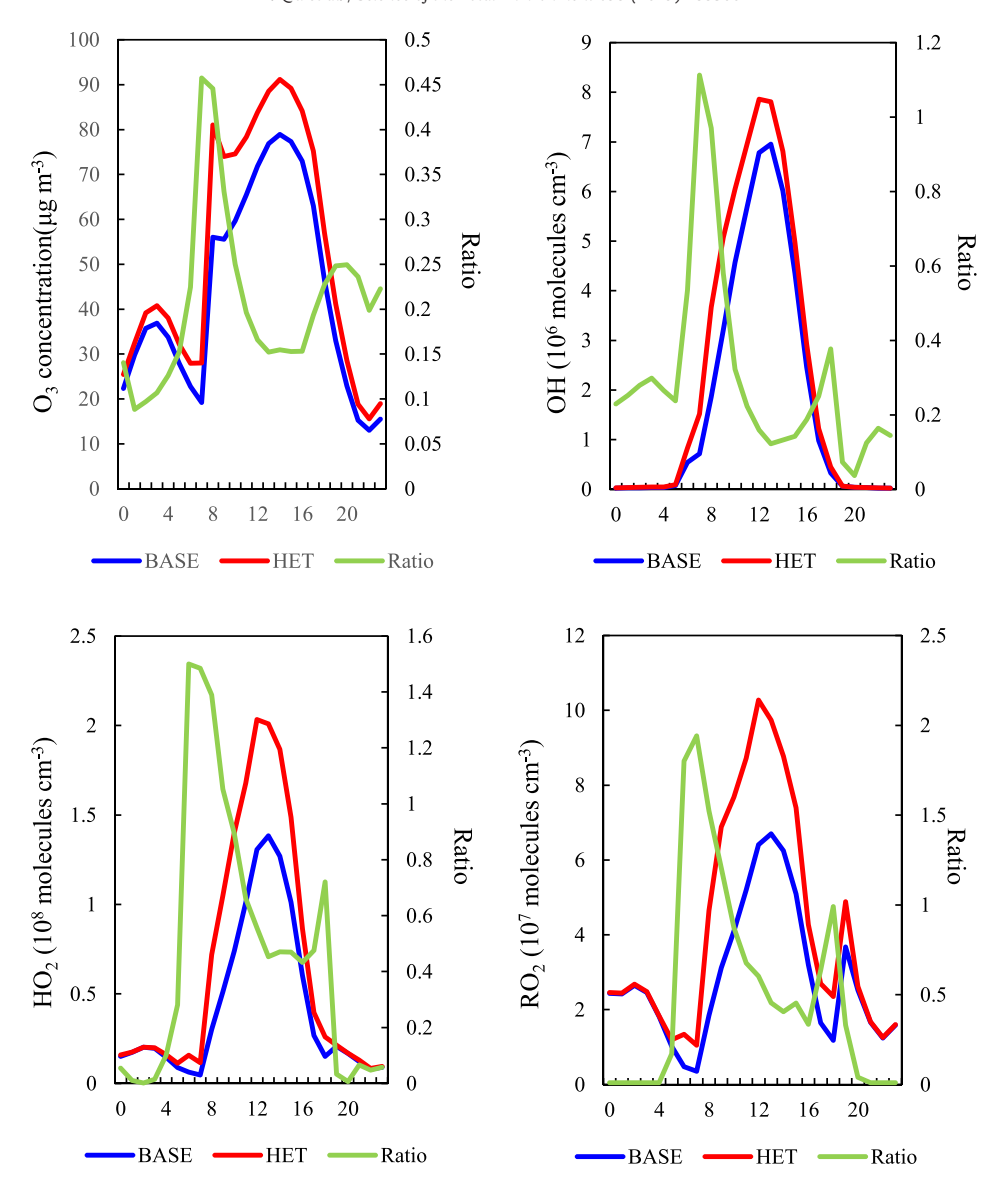


Fig. 3. Simulated averaged hourly  $O_3$ , OH,  $HO_2$  and  $RO_2$  concentrations in July 2014 and the relative changes between original (BASE case) and improved CMAQ (HET case). Ratio = (HET-BASE)/BASE. The results are based on hourly concentrations at the position in the red circle in Fig. 2(j).

of  $Cl^{\bullet}$  from  $ClNO_2$  and  $Cl_2$  were estimated directly using observation data (Liu et al., 2017), previous modeling studies have not considered all heterogeneous reactions included in this study and thus could lead to more biases in their evaluation of the  $Cl^{\bullet}$  sources.

A zero-out method, which deactivates the heterogeneous reactions one at a time, is used to quantify the contributions to Cl• from the photolysis of Cl₂ (from heterogeneous uptakes of O₃, OH, HOCl, ClNO₂, and ClONO₂), ClNO₂ (from heterogeneous uptake of N₂O₅) and ClNO (from heterogeneous uptake of NO₂). The difference between a specific zero-out case and the HET case is considered as the contributions from the heterogeneous reaction that is turned off in the simulation. The nonlinearity of these heterogeneous reactions on Cl₂ and Cl• is rather small. The sum of the contribution of each chemical reaction to Cl• using the zero-out method is generally equal to the total concentrations predicted by the HET case, with a relative difference of approximately 5%

Fig. 4 shows that both the photolysis of ClNO<sub>2</sub> and Cl<sub>2</sub> are important contributors (42.4% and 57.6%, respectively) to atmospheric Cl• in the early morning hours from of 5:00 to 8:00 but the photolysis of Cl<sub>2</sub> is the only significant source of Cl• after 10:00. This is because ClNO<sub>2</sub> production from N<sub>2</sub>O<sub>5</sub> uptake mainly occurs at night and there is no

significant continuous source of  $CINO_2$  in the daytime due to low  $N_2O_5$  concentrations. In contrast,  $Cl_2$  forms continually because of excess  $O_3$ . These results indicate that 3D CTM modeling studies without the  $O_3$  heterogeneous reaction with PCl likely underestimated the atmospheric  $Cl^{\bullet}$  as well as OH,  $HO_2$ , and  $RO_2$ . It is worth mentioning that  $Cl_2$  from the heterogeneous uptake of  $CINO_2$  to is negligible because the pH of the particle seldom goes below 2 (Fig. S3), which is the acidity required for R9 to occur. The predicted high aerosol pH also agrees with a few field studies (Pan et al., 2018; Guo et al., 2017).

The contributions to  $\text{Cl}_2$  from heterogeneous production of  $\text{O}_3$ , OH,  $\text{CINO}_2$ ,  $\text{CIONO}_2$ , and HOCI on PCI are also quantified in July 2014. The heterogeneous reactions of  $\text{O}_3$  (R4) are the most important source of  $\text{Cl}_2$  (81%). The reactions of OH (R5–6, 6.4%) and  $\text{CIONO}_2$  (R7, 7.4%) also have significant contributions. In general, heterogeneous reactions of  $\text{CINO}_2$  and HOCI have only small additional contributions to  $\text{Cl}_2$  (2.2% and 3%, reactively). The photolysis of  $\text{CINO}_2$  from R3 is only important during the early morning hours (40%) but has almost negligible contributions during daytime hours (see Fig. 4). Since these additional reactions lead to significantly higher  $\text{Cl}_2$  concentrations, previous works without these reactions likely significantly underestimated the Cl• and thus the impact

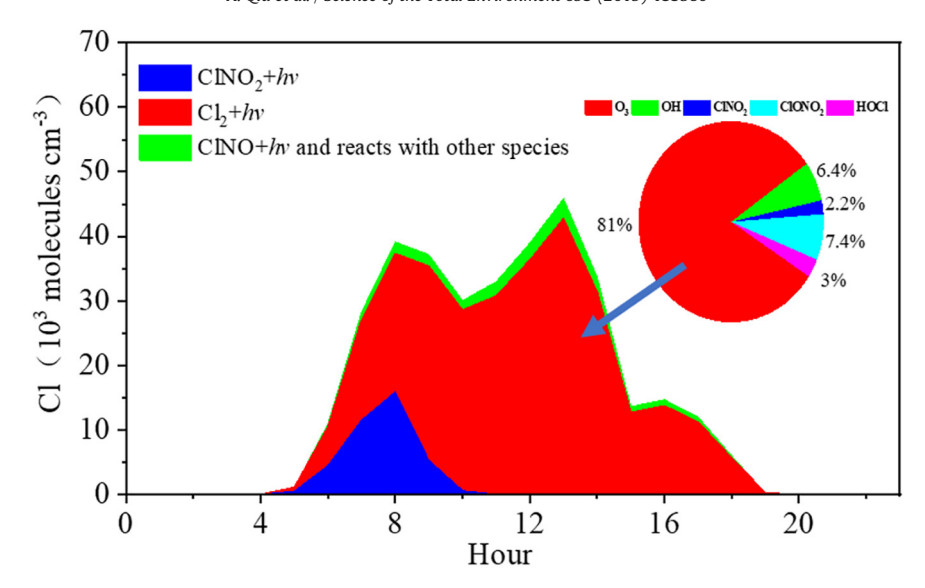


Fig. 4. Quantifications of hourly chlorine radical from the photolysis of Cl<sub>2</sub>, CINO<sub>2</sub> and CINO, and from other gaseous species at Wangdu. The contributions of heterogeneous reactions of O<sub>3</sub>, OH, CINO<sub>2</sub>, CIONO<sub>2</sub> and HOCl to predicted Cl<sub>2</sub> concentrations are shown as the inset pie chart. The results are based on hourly concentrations at Wangdu in July 2014 for the HET case.

of chlorine on the oxidation of VOCs and the formation of  $RO_2$  and  $HO_2$  radicals from these reactions. As recent chamber studies showed that oxidation of VOCs by Cl could also be a potential source of secondary organic aerosol (Wang and Ruiz, 2017), neglecting these reactions could lead to underestimation of the contribution of Cl on SOA formation in the regional CTMs.

## 4. Discussion

# 4.1. Potential cause of model underpredictions and overpredictions of chlorine species

To the best knowledge of the authors, this study is the first study to compare modeled and observed  $\text{Cl}_2$  in a polluted urban region using a 3D CTM. Simulated  $\text{Cl}_2$  and  $\text{ClNO}_2$  levels from the HET case are still substantially higher or lower than the observations. One of the uncertainties in the model parameters is the uptake coefficients. As  $\text{N}_2\text{O}_5$  are important precursors of  $\text{ClNO}_2$ , the sensitivity simulations that with the  $\text{N}_2\text{O}_5$  parameterization from Davies et al. input are conducted, Fig. S4 shows that in both Wangdu and IAP, the alternative  $\text{N}_2\text{O}_5$  parameterization from Davis et al. does not lead to much change in  $\text{Cl}_2$  (neither in  $\text{ClNO}_2$ , not shown in Fig. S4). The overprediction of  $\text{Cl}_2$  may be associated with a very large uptake coefficient, e.g. the hypothetical value used in the present study ( $10^{-3}$  as suggested by Keene et al., 1990) have not been confirmed and is required to reproduce the observed level of  $\text{Cl}_2$  in the ambient air.

Another important source of uncertainty is the particle surface area. The capability of the CMAQ model in predicting particle surface area (PSA) concentrations is much less studied than its ability in predicting particle mass concentrations. As there is no direct measurement of PSA at Wangdu, the predicted hourly particulate surface area at the IAP site are compared with measurements reported in Zhou et al. (2018), as shown in Fig. S5(a). The CMAQ model appears to significantly underpredicted PSA at night by a factor of 7-8 and a factor of 3-4 during the day even though the dry mass concentrations are well predicted. The CMAQ model might under-estimated the Aitken mode particles, which contributes little mass but could contribute more in surface area, or underestimate the water content of the aerosols, which can affect their size. On the other hand, the observed PSA was based on measured number size distribution and converted to wet PSA using growth factors, which may subject to large uncertainties as well. However, it is without question that PSA is underpredicted in the current study. An additional sensitivity simulation is conducted by increasing the calculated surface area by a factor of 3 during the day (0800–2000) and a factor of 8 for the rest of the hours. This resulted in significantly higher ClNO<sub>2</sub> concentrations in both Wangdu and IAP (Fig. S5(b)) and improved model performance (Table S4). More studies are needed in the future to evaluate and improve the capability of the CMAQ model in predicting particle surface areas.

PCl and NOx emission and transport can also affect the predicted  $\text{Cl}_2$  and  $\text{ClNO}_2$  concentrations. The NCP region has high PCl emissions and PCl in the HET case is not depleted (see Fig. S6), indicating that the PCl concentration is not a limiting factor in determining the  $\text{Cl}_2$ ,  $\text{ClNO}_2$ , and other gaseous chlorine species. A sensitivity simulation which increases the PCl emission by a factor of 2 in the entire domain only leads to 5–10% increases in the  $\text{Cl}_2$  and  $\text{ClNO}_2$  concentrations. The NOx emissions in the NCP region have been subjected to many previous studies and are relatively accurate (Cai et al., 2017). Model performance for  $\text{NO}_2$  and other species in the NCP (see Table S2) further confirms this. Thus, it is expected that mixing and regional transport of NOx are well captured in the model and is not a major factor that affects the accuracy of the predicted  $\text{Cl}_2$  and  $\text{ClNO}_2$  concentrations.

# 4.2. Implications

Taking the north China as an example, this work showed that the concentrations of ozone and free radicals can increase by various extents (averaged by 20%, 28%, 36% and 48% for O<sub>3</sub>, OH, HO<sub>2</sub> and RO<sub>2</sub> for some regions in southern BTH area) due to inclusion of seven heterogeneous reactions that generate reactive chlorine species, proving that chlorine heterogeneous chemistry has a significant impact on atmospheric ozone and free radical formation. In particular, the inclusion of several of these heterogeneous reactions on chlorinated particles that generate Cl<sub>2</sub>, especially the one with O<sub>3</sub>, can explain the observed Cl<sub>2</sub> concentrations and the strong correlation between elevated O<sub>3</sub> and Cl<sub>2</sub> concentrations in the field. These results suggest that previous 3D modeling studies without these reactions were likely significantly underestimated the Cl radical concentrations and thus the impact of chlorine on the oxidation of VOCs and the formation of RO2 and HO2 radicals from these reactions. Box model simulations constrained by observations should also be reexamined to assess the impact of these additional reactions.

In addition, recent chamber studies showed that oxidation of VOCs by Cl could also be a potential source of secondary organic

aerosol (Wang and Ruiz, 2017), neglecting these reactions could lead to underestimation of the contribution of Cl on SOA formation in the regional CTMs. Our study also suggests that the on-going NO<sub>x</sub> emission controls in the NCP region with a goal to reduce both O<sub>3</sub> and secondary nitrate can also have the co-benefit of reducing the formation Cl• from ClNO2 and Cl2, which may also lead to lower secondary organic aerosol formation and thus the control of summertime PM<sub>2.5</sub> in the region.

#### Acknowledgments

This work was supported by National Natural Science Foundation of China (21625701), China Postdoctoral Science Foundation (2018M641385), National Research Program for Key Issue in Air Pollution Control (DQGG0301, DQGG0501) and National Key Research and Development Program of China (2018YFC0213805, 2018YFC0214006). The simulations were completed on the "Explorer 100" cluster system of Tsinghua National Laboratory for Information Science and Technology.

## Appendix A. Supplementary data

Supplementary data to this article can be found online at https://doi. org/10.1016/j.scitotenv.2019.133580.

#### References

- Abbatt, J.P.D., Waschewsky, G.C.G., 1998. Heterogeneous interactions of HOBr, HNO<sub>3</sub>, O<sub>3</sub>, and NO2 with deliquescent NaCl aerosols at room temperature. J. Phys. Chem. A
- Behnke, W., Zetzsch, C., 1989. Heterogeneous formation of chlorine atoms from various aerosols in the presence of O<sub>3</sub> and HCl. J. Aerosol Sci. 20, 1167-1170.
- Bertram, T.H., Thornton, J.A., 2009. Toward a general parameterization of N<sub>2</sub>O<sub>5</sub> reactivity on aqueous particles: the competing effects of particle liquid water, nitrate and chloride. Atmos. Chem. Phys. 9 (2009), 8351-8363
- Butchart, N., Scaife, A.A., 2001. Removal of chlorofluorocarbons by increased mass exchange between the stratosphere and troposphere in a changing climate. Nature
- Cai, S.Y., Wang, Y.J., Zhao, B., et al., 2017. The impact of the "Air Pollution Prevention and Control Action Plan" on PM<sub>2.5</sub> concentrations in Jing-Jin-Ji region during 2012–2020. Sci. Total Environ. 580 (2017), 197–209.
- Chang, X., Wang, S.X., Zhao, B., et al., 2017. Assessment of inter-city transport of particulate matter in the Beijing-Tianjin-Hebei region. Atmos. Chem. Phys. 18, 1-28
- Davis, J.M., Bhave, P.V., Foley, K.M., 2008. Parameterization of N<sub>2</sub>O<sub>5</sub> reaction probabilities on the surface of particles containing ammonium, sulfate, and nitrate. Atmos. Chem. Phys. 8 (2008), 5295-5311.
- Deiber, G., George, C., LeCalve, S., et al., 2004. Uptake study of CIONO2 and BrONO2 by Halide containing droplets. Atmos. Chem. Phys. 4, 1291-1299.
- Faxon, C.B., Bean, J.K., Hildebrandt, R.L., 2015. Inland concentrations of Cl2 and ClNO2 in Southeast Texas suggest chlorine chemistry significantly contributes to atmospheric reactivity. Atmosphere 6 (2015), 1487-1506.
- Finlayson-pitts, B.J., Ezell, M.J., Pitts, J.N., 1989. Formation of chemically active chlorine compounds by reactions of atmospheric NaCl particles with gaseous N2O5 and ClONO<sub>2</sub>. Nature 337, 241-244.
- Finley, B.D., Saltzman, E.S., 2006. Measurement of Cl<sub>2</sub> in coastal urban air. Geophys. Res. Lett. 33 (2006), 203-362.
- Fu, X., Wang, T., Wang, S.X., et al., 2018. Anthropogenic emissions of hydrogen chloride and fine particulate chloride in China. Environ Sci Technol 52, 1644-1654
- Gebel, M.E., Finlayson-Pitts, B.J., 2001. Uptake and reaction of ClONO2 on NaCl and synthetic sea salt. J. Phys. Chem. A 105, 5178-5187.
- George, I.J., Abbatt, J.P.D., 2010. Heterogeneous oxidation of atmospheric aerosol particles by gas-phase radicals, Nat. Chem. 2 (2010), 713-722.
- Graedel, T.E., Keene, W.C., 1995. Tropospheric budget of reactive chlorine. Global Biogeochem Cy 9, 47-77.
- Guo, H.Y., Weber, R.J., Nenes, A., et al., 2017. High levels of ammonia do not raise fine particle pH sufficiently to yield nitrogen oxide-dominated sulfate production. Sci. Rep. 7,
- Keene, W.C., Pszenny, A.A.P., Jacob, D.J., et al., 1990. The geochemical cycling of reactive chlorine through the marine troposphere. Global Biogeochem Cy 4 (1990), 407–430.
- Keene, W.C., Khalil, M.A.K., Erickson, D.J., et al., 1999. Composite global emissions of reactive chlorine from anthropogenic and natural sources; reactive chlorine emissions inventory. J. Geophys. Res.-Atmos. 104, 8429–8440.
- Knipping, E.M., Lakin, M.J., Foster, K.L., et al., 2000. Experiments and simulations of ionenhanced interfacial chemistry on aqueous NaCl aerosols. Science 288 (2000), 301-306

- Laskin, A., Wang, H., Robertson, W.H., et al., 2006, A new approach to determining gasparticle reaction probabilities and application to the heterogeneous reaction of deliquesced sodium chloride particles with gas-phase hydroxyl radicals. J. Phys. Chem. 110 (2006), 10619–10627.
- Li, Q.Y., Zhang, L., Wang, T., Tham, Y.J., Ahmadov, R., Xue, L.K., Zhang, Q., Zheng, J.Y., 2016. Impacts of heterogeneous uptake of dinitrogen pentoxide and chlorine activation on ozone and reactive nitrogen partitioning; improvement and application of the WRF-Chem model in southern China, Atmos. Chem. Phys. 16 (2016), 14875–14890.
- Li, Z., Jiang, J.K., Ma, Z.Z., et al., 2017. Influence of flue gas desulfurization (FGD) installations on emission characteristics of PM<sub>2.5</sub> from coal-fired power plants equipped with selective catalytic reduction (SCR), Environ, Pollut, 230, 655-662.
- Liao, J., Huey, G., Liu, Z., et al., 2014. High levels of molecular chlorine in the Arctic atmo-
- sphere, Nat. Geosci. 7 (2014), 91–94. Liu, X.X., Qu, H., Huey, L.G., Wang, Y.H., et al., 2017. High levels of daytime molecular chlorine and nitryl chloride at a rural site on the North China Plain. Environ Sci Technol 51 9588-9595
- McDuffie, E.E., Fibiger, D.L., Dubé, W.P., et al., 2018. Heterogeneous N<sub>2</sub>O<sub>5</sub> uptake during Winter: aircraft measurements during the 2015 WINTER campaign and critical evaluation of current parameterizations. J. Geography. Res. Atmos. 123, 4345-4372.
- Osthoff, H.D., Roberts, J.M., Ravishankara, A.R., et al., 2008. High levels of nitryl chloride in the polluted subtropical marine boundary layer. Nat. Geosci. 1, 324-328.
- Oum, K.W., Lakin, M.J., DeHaan, D.O., et al., 1998. Formation of molecular chlorine from the photolysis of ozone and aqueous sea-salt particles. Science 279, 74-77.
- Pan, Y.P., Tian, S.L., Liu, D.W., et al., 2018. Source apportionment of aerosol ammonium in an ammonia-rich atmosphere: an isotopic study of summer clean and hazy days in urban Beijing. J. Geophys. Res. Atmos. 10, 5681-5689.
- Pratte, P., Rossi, M.J., 2006. The heterogeneous kinetics of HOBr and HOCl on acidified sea salt and model aerosol at 40-90% relative humidity and ambient temperature. Phys. Chem. Chem. Phys. 8, 3988-4001.
- Qiu, X.H., Duan, L., Chai, F.H., et al., 2016. Deriving high-resolution emission inventory of open biomass burning in China based on satellite observations. Environ Sci Technol 50, 11779-11786.
- Qiu, X.H., Ying, Q., Wang, S.X., et al., 2019. Modeling the impact of heterogeneous reactions of chlorine on summertime nitrate formation in Beijing, China. Atmos.Chem. Phys. 19, 6737-6747.
- Riedel, T.P., Bertram, T.H., Crisp, T.A., Williams, E.J., et al., 2012. Nitryl chloride and molecular chlorine in the coastal marine boundary layer. Environ Sci Technol 46, 10463-10470
- Roberts, J.M., Osthoff, H.D., Brown, S.S., Ravishankara, A.R., 2008. N<sub>2</sub>O<sub>5</sub> oxidizes chloride to Cl<sub>2</sub> in acidic atmospheric aerosol. Science 321, 1059.
- Roberts, J.M., Osthoff, H.D., Brown, S.S., et al., 2009. Laboratory studies of products of N<sub>2</sub>O<sub>5</sub> uptake on Cl<sup>-</sup> containing substrates. Geophys. Res. Lett. 36, L20808.
- Rossi, M.J., 2003. Heterogeneous reactions on salts. Chem. Rev. 103, 4823-4882.
- Sander, R., Crutzen, P.J., 1996. Model study indicating halogen activation and ozone destruction in polluted air masses transported to the sea. J. Geophys. Res.-Atmos. 101,
- Sarwar, G., Simon, H., Bhave, P., et al., 2012. Examining the impact of heterogeneous nitryl chloride production on air quality across the United States. Atmos. Chem. Phys. 12, 6455-6473.
- Sarwar, G., Simon, H., Xing, J., et al., 2014. Importance of tropospheric CINO2 chemistry across the Northern Hemisphere. Geophys. Res. Lett. 41, 4050-4058.
- Shen, G.F., Yang, Y.F., Wang, W., et al., 2010. Emission factors of particulate matter and elemental carbon for crop residues and coals burned in typical household stoves in China. Environ Sci Technol 44, 7157-7162
- Simon, H., Kimura, Y., GcGaughey, G., et al., 2009. Modeling the impact of CINO2 on ozone formation in the Houston area. J. Geography. Res. Atmos. https://doi.org/10.1029/
- Tan, Z.F., Fuchs, H., Lu, K.D., et al., 2017. Radical chemistry at a rural site (Wangdu) in the North China Plain: observation and model calculations of OH, HO2 and RO2 radicals. Atmos. Chem. Phys. 17, 663-690.
- Thornton, J.A., Abbatt, J.P.D., 2005. N<sub>2</sub>O<sub>5</sub> reaction on submicron sea salt aerosol: kinetics, products, and the effect of surface active organics. J. Phys. Chem. A 109, 10004-10012.
- Thornton, J.A., Kercher, J.P., Riedel, T.P., et al., 2010. A large atomic chlorine source inferred from mid-continental reactive nitrogen chemistry. Nature 464,
- Von Glasow, R., 2010. Atmospheric chemistry: wider role for airborne chlorine. Nature 464 (7286), 168-169.
- Wang, D.S., Ruiz, L.H., 2017. Secondary organic aerosol from chlorine-initiated oxidation of isoprene. Atmos. Chem. Phys. 17, 13491-13508.
- Wang, L., Arey, J., Atkinson, R., 2005. Reactions of chlorine atoms with a series of aromatic hydrocarbons. Environ Sci Technol 39, 5302-5310.
- Wang, L.L., Thompson, T., McDonald-Buller, E.C., et al., 2007. Photochemical modeling of emissions trading of highly reactive volatile organic compounds in Houston, Texas. 1. Reactivity-based trading and potential for ozone hot spot formation. Environ Sci Technol 41, 2095-2102.
- Wang, T., Tham, Y.J., Xue, L.K., et al., 2016. Observations of nitryl chloride and modeling its source and effect on ozone in the planetary boundary layer of southern China. J. Geography. Res. Atmos. 121, 2476–2489.
- Ying, Q., Li, J.Y., Kota, S.H., 2015. Significant contributions of isoprene to summertime secondary organic aerosol in eastern United States. Environ Sci Technol 49, 7834-7842.
- Young, C.J., Washenfelde, R.A., Edwards, P.M., et al., 2014. Chlorine as a primary radical: evaluation of methods to understand its role in initiation of oxidative cycles. Atmos. Chem. Phys. 14, 3427-3440.
- Yu, S., Mathur, R., Sarwar, G., et al., 2010. Eta-CMAQ air quality forecasts for O<sub>3</sub> and related species using three different photochemical mechanisms (CB4, CB05, SAPRC-99):

- comparisons with measurements during the 2004 ICARTT study. Atmos. Chem. Phys. 10, 3001–3025.
- Zhang, Q.Y. Li, Wang, T., Ahmadov, R., et al., 2017. Combined impacts of nitrous acid and nitryl chloride on lower-tropospheric ozone: new module development in WRF-Chem and application to China. Atmos. Chem. Phys. 17, 9733–9750.
   Zhao, B., Jiang, J.H., Diner, D.J., et al., 2018. Intra-annual variations of regional aerosol optical depth, vertical distribution, and particle types from multiple satellite

- and ground-based observational datasets. Atmos. Chem. Phys. 18, 11247–11260. Zhou, W., Zhao, J., Ouyang, B., et al., 2018. Production of  $N_2O_5$  and  $CINO_2$  in summer in urban Beijing, China. Atmos. Chem. Phys. 18, 11581–11597.